PHYSICAL REVIEW B **92**, 140415(R) (2015)

Experimental observation of multiple-Q states for the magnetic skyrmion lattice and skyrmion excitations under a zero magnetic field

Masahiro Nagao,[1,2,*] Yeong-Gi So,[3] Hiroyuki Yoshida,[4] Kazunari Yamaura,[5] Takuro Nagai,[2] Toru Hara,[2] Atsushi Yamazaki,[1] and Koji Kimoto[2]

[1]*Department of Resources and Environmental Engineering, School of Creative Science and Engineering, Waseda University, Shinjuku, Tokyo 169-8555, Japan*

[2]*Electron Microscopy Group, Surface Physics and Structure Unit, National Institute for Materials Science, Tsukuba, Ibaraki 305-0044, Japan*

[3]*Department of Materials Science and Engineering, Faculty of Engineering and Resource Science, Akita University, Akita, Akita 010-8502, Japan*

[4]*Department of Physics, Faculty of Science, Hokkaido University, Sapporo, Hokkaido 060-0810, Japan*

[5]*Superconducting Properties Unit, National Institute for Materials Science, 1-1 Namiki, Tsukuba, Ibaraki 305-0044, Japan*

(Received 13 August 2015; revised manuscript received 10 October 2015; published 27 October 2015)

Model calculations indicate that the magnetic skyrmion lattice (SkL) is represented by a superposition of three spin helices at an angle of 120° to each other, the so-called triple-Q state. Using Lorentz transmission electron microscopy, we investigated the relationship between the SkL and the helix in FeGe thin films. After the magnetic field is removed, the ordered skyrmions are trapped inside helimagnetic domain walls (HDWs) where the different helical Q vectors are encountered. *In situ* observation revealed an unexpected topological excitation under such a zero-field state: skyrmions are spontaneously formed at HDWs.

DOI: 10.1103/PhysRevB.92.140415 PACS number(s): 75.70.Kw, 68.37.Lp, 75.30.Kz, 75.50.−y

Magnetic skyrmions are topologically stable particlelike objects. In B20-type chiral-lattice magnets with cubic $P2_13$ symmetry such as MnSi, $Fe_{1-x}Co_xSi$, and FeGe, their spin configuration is a vortexlike spin swirling oriented in all directions, characterized by a topological charge of $S = 1$, which is defined as a measure of the magnetization curvature [1–9]. At zero magnetic field, such magnets show helical spin order, the so-called single-Q state where the spin configurations are trivial ($S = 0$), as illustrated in Fig. 1(a). When an external magnetic field (B) is applied, the triangular skyrmion lattice (SkL) is stabilized by the Dzyaloshinskii-Moriya interaction [1–9]. Owing to their topological nature, magnetic skyrmions have attracted much attention in both applications [9–13] and fundamental sciences [14–19]. Examples are the topological Hall effect [10] and the movement of the SkL by an electric current of ultralow density [11,12], which are associated with the emergent magnetic field caused by the integral topological charge. In addition, SkLs are considered the most prominent candidate for an unusual magnetic state with "partial order" that occurs under high pressure in MnSi, and their excitations are supposed to drive a breakdown of Fermi liquid theory [14–19].

The pioneering theoretical work on magnetic topological solitons including skyrmions was performed in references such as [1–4]. Subsequently, in conjunction with the experimental discovery of the SkL, model calculations indicated that the triangular SkL state is represented by a superposition of three helices at an angle of 120° to each other in a plane, the so-called triple-Q state [5], as depicted in Fig. 1(b). Mühlbauer *et al.* discussed the quartic term in the Ginzburg-Landau free energy in the mean-field approximation [5]. When an external magnetic field is applied, the quartic term leads to cubic interactions in the magnetization which stabilize the three helices with Q vectors normal to $\boldsymbol{B}$. The SkL is characterized by the magnetization

$$\boldsymbol{M}(\boldsymbol{r}) \approx \boldsymbol{M}_{\mathrm{uniform}} + \sum_{i=1}^{3} \boldsymbol{M}_{Q_i}(\boldsymbol{r} + \Delta \boldsymbol{r}_i)$$

where $\boldsymbol{M}_{Qi}(\boldsymbol{r}) = A[\boldsymbol{M}_{i1}\cos(\boldsymbol{Q}_i \cdot \boldsymbol{r}) + \boldsymbol{M}_{i2}\sin(\boldsymbol{Q}_i \cdot \boldsymbol{r})]$ is the magnetization of a single helix with amplitude A, and M_{uniform} is the uniform magnetization induced by the Zeeman effect [5,9]. The three Q vectors normal to $\boldsymbol{B}$ add up to zero, forming angles of 120° with each other.

On the basis of the triple-Q model, theoretical analyses have described and predicted various excitation modes of the SkL, such as current-driven collective motion [20,21], rotational spin-wave modes [22,23], and phason excitations [24]. In addition, several theoretical studies have explored formation of the SkL as the cause of the partial order in the non-Fermi-liquid (NFL) state [14–16]. However, experimental evidence of the triple-Q model as the hybridization state of helical Q vectors is scarce. In other words, little is known of the relationship between the SkL and helical spin order states, although it is very important for applications and fundamental sciences.

In this Rapid Communication, using Lorentz transmission electron microscopy (LTEM), we show the relationship between the SkL and helical spin order states by examining a first-order transition from the SkL to helimagnetic phases. Specifically, we observed the spatial distributions of the metastable skyrmions in the helimagnetic phase of FeGe thin films under a zero-field state after removing the magnetic field. Our LTEM images demonstrated that the ordered skyrmions are trapped inside helimagnetic domain walls (HDWs) where the different helical Q vectors are encountered. Moreover, *in situ* observation revealed skyrmion excitations at HDWs under such a zero-field state, caused by thermal fluctuation and a force that stabilizes skyrmions by the proliferation of topological defects.

Polycrystals of FeGe were synthesized by arc melting and a high-pressure treatment with the same procedure as in

*m.nagao@aoni.waseda.jp

 ©2015 American Physical Society

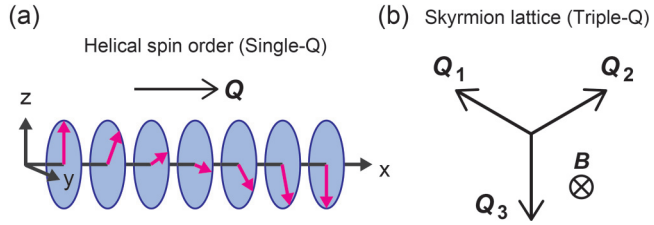

FIG. 1. (Color online) (a) Depiction of the spin configurations in helical spin order, the so-called single-Q state. Q is the propagation vector of the helix. (b) Depiction of the triple-Q state for the SkL.

Ref. [25]. The observations were carried out using an LTEM system operated at 300 kV. The thin films were prepared by argon-ion milling after a mechanical polishing process. The magnetic field applied normal to the thin plate was induced by the magnetic objective lens of the TEM system [7,8]. We used the Fresnel method to image the skyrmions and helices. The magnetic distributions obtained by the Fresnel method were analyzed using the software QPT for DIGITALMICROGRAPH, which enabled us to compute the phase changes of electron waves and the components of the magnetization normal to the electron propagation direction on the basis of the transport-of-intensity equation [26].

The magnetic field dependence of the magnetic structures is presented in Figs. 2(a)–2(d). This observed area is a single grain, and becomes thinner from upper right to lower left because we used the wedge-shaped thin films prepared by the argon-ion milling. In Fig. 2(a), the SkL, shown as the triangular array of bright dots [7,8], almost persists down to $T = 200$ K under $B = 100$ mT. As B is reduced to 85 mT, the SkL regions begin a withdrawal from the thicker regions [Fig. 2(b)]. This is because at a low temperature away from the magnetic transition temperature T_C of 273 K for FeGe thin films [25,27] skyrmions are unstable in thicker regions [8]. Simultaneously, periodic stripe lines orthogonal to the helical Q-vector direction [28,29] begin to grow. A decrease in B to 60 mT promotes growth in the stripe regions [Fig. 2(c)]. Additionally, the stripes grow in a different direction in the lower right region. At $B = 0$ mT [Fig. 2(d)], the stripes finally become the dominant state. However, some of the skyrmions survive as a metastable state in the helimagnetic phase, as indicated by the circles in Fig. 2(d). The coexistence of the skyrmion state and helical or conical states was observed with increasing B in different chiral magnets [6,30–33]. The lower contrast of the stripes in Figs. 2(a)–2(c) implies a helicoid structure as theoretically predicted [34]. In the subsequent experiments, all the images were obtained in the same way as Fig. 2(d).

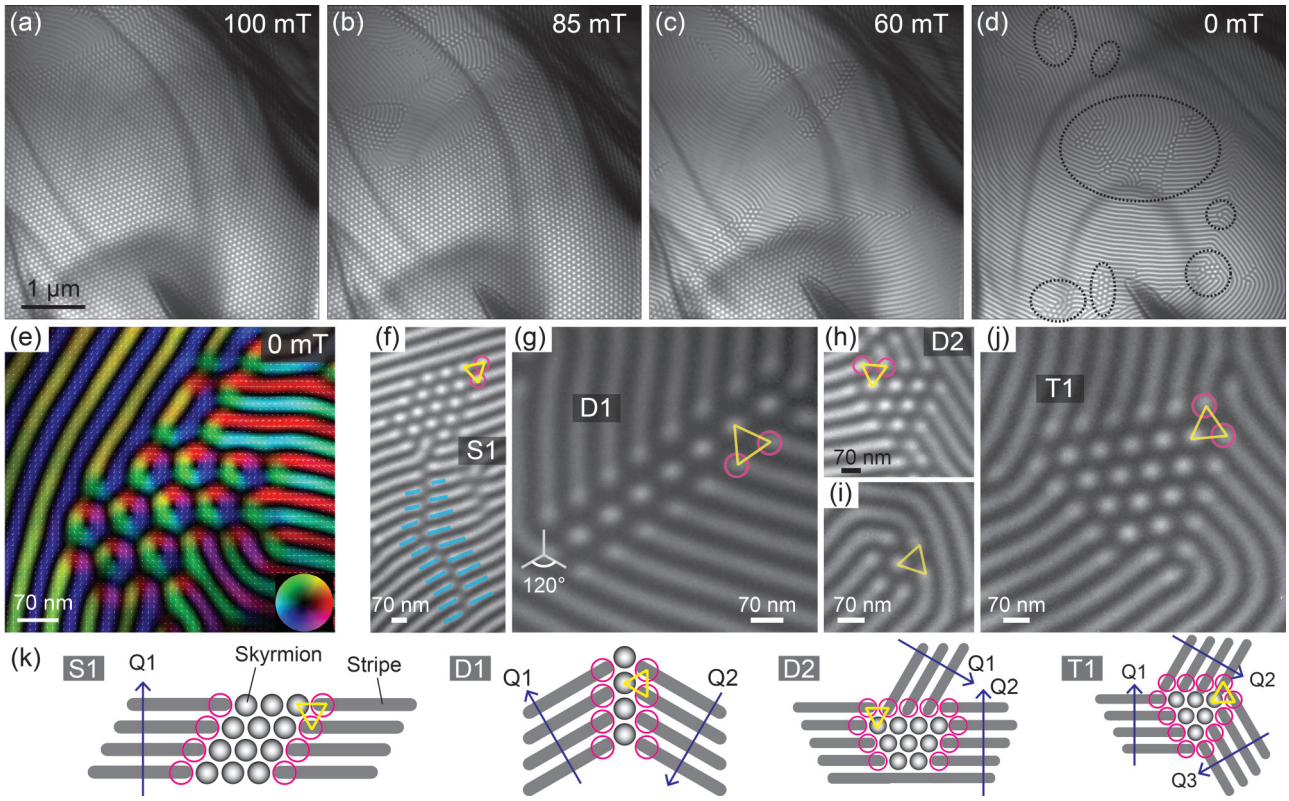

FIG. 2. (Color online) (a)–(d) Series of Fresnel images at 200 K with decreasing B from 100 mT to 0 mT. In (d), the metastable skyrmions are circled with dashed lines. The knife-shaped dark contrast in the lower region is a contaminant. (e) Magnetization distribution map at 200 K under a zero field after removing the field of 100 mT. The magnetization direction at every point is represented by the inset color wheel. (f)–(j), Fresnel images obtained from various regions. The labels S1, D1, D2, and T1 refer to the classification schematics in (k). The magenta circles are superimposed on the meronlike stripe terminations. The yellow triangles are comprised of skyrmions and the stripe terminations. In (f), the light-blue lines are drawn along the stripes. (k) Classification schematics of the relationship between the skyrmions and stripes. The magenta circles and yellow triangles have the same meaning as in (f)–(j).

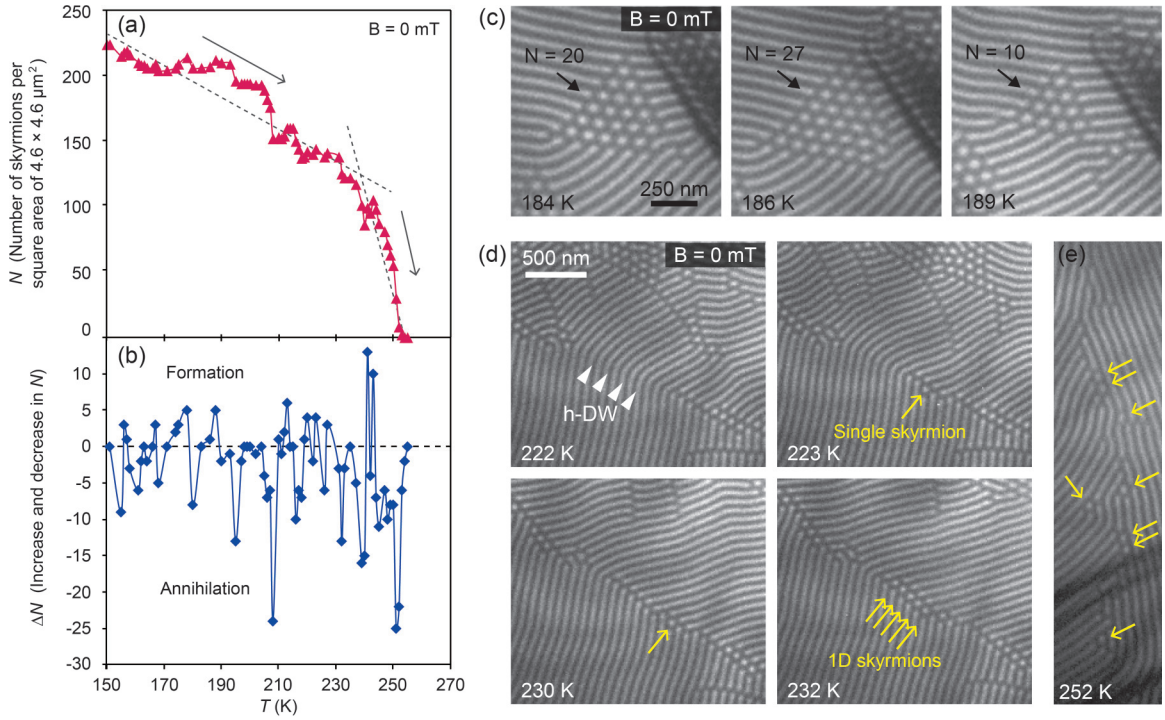

FIG. 3. (Color online) (a) Change in the number of metastable skyrmions (N) with increasing T. The dashed lines are a visual guide. (b) Increase and decrease in N. ΔN is obtained by subtracting N at a given temperature from that at the next temperature in (a). (c),(d) Series of Fresnel images under a zero field with increasing T. In (d), the white triangular arrows and yellow arrows indicate the HDW and the spontaneously formed skyrmions, respectively. (e) Fresnel image obtained at 252 K just prior to the disappearance of skyrmions by heating shown in (a). The yellow arrows indicate the last skyrmions.

Figure 2(e) shows a magnetization distribution map. The array of skyrmions maintains the triangular lattice. In addition, a bimeronlike spin texture as theoretically predicted [35,36], which is topologically equivalent to skyrmions, is located above the ordered skyrmion cluster. The cluster exists beside the meronlike (half-skyrmion-like) structure of stripe terminations including one end of the bimeron, and is surrounded by stripes with different Q-vector directions. Such skyrmions are closely correlated with the stripe structures which are classified into four types, as follows. The Fresnel images obtained from various regions are presented in Figs. 2(f)–2(j). The labels S1, D1, D2, and T1 refer to the classification schematics in Fig. 2(k). Skyrmions are infrequently located in the straight stripes (S1 type), as shown in Fig. 2(f). The magenta circles are superimposed on the stripe terminations. The triangular array comprising skyrmions and stripe terminations is shown, as highlighted by the yellow triangles. In Figs. 2(g) and 2(h), skyrmions are located in the double-Q-type HDWs. In Fig. 2(g), the angle between the two stripes is approximately 120° at the HDW (D1 type). The image clearly shows a one-dimensional (1D) skyrmion array which is often observed at the 120° HDWs. Figure 1(h) shows skyrmions located in a conventional HDW (D2 type) [8,29]. In both the D1 and D2 types, as well as the S1 type, the skyrmions and stripe terminations constitute triangular arrays. Fresnel images of a single skyrmion and skyrmions located in the triple-Q-type HDW (T1 type) are presented in Figs. 2(i) and 2(j), respectively. The triangular array rule is also obeyed. These results show that skyrmions can exist when the meronlike stripe terminations are placed at the triangular lattice points. In the lower region of Fig. 2(f), there is a linear helimagnetic domain boundary (HDB) comprising an incomplete antiphase boundary, which was not observed in the zero-field cooling state. It is possible that the HDB is a vestige of 1D skyrmions that broke the triangular array rule. With the exception of the S1 type and single skyrmions, the clusters always remain in roughly the same location but their morphology and size vary. This may be due to atomic lattice defects, impurities, and the stress-strain field. However, these are indirect causes. The main reason is the hysteretic nucleation and growth process of the helimagnetic phase, because the helimagnetic phase always has the same structure with small variations in the details [37], and skyrmions are finally trapped in HDWs where the different Q vectors are encountered. Note that, in our FeGe thin films, the helimagnetic domain structure shows little change with temperature change [37], in contrast to the bulk [38].

In epitaxial FeGe(111) thin films, Huang and Chien have detected the sign of the topological Hall resistivity under a zero magnetic field after removing the field [27]. They speculated that the sign of the topological Hall resistivity at zero field arises from the pinning of skyrmions by the grain boundaries (GBs). Our real-space observations indicate that skyrmions at HDWs should make a large contribution to the topological Hall resistivity, rather than skyrmions pinned to the GBs.

We investigated the response of the metastable skyrmions to an increase in temperature. Figure 3(a) shows the change in the metastable skyrmion density per the square area of 4.6×4.6 μm^2 with increasing T under a zero field. In the observed area, there are a large number of the metastable skyrmions at 150 K. As T is increased from 150 to 237 K,

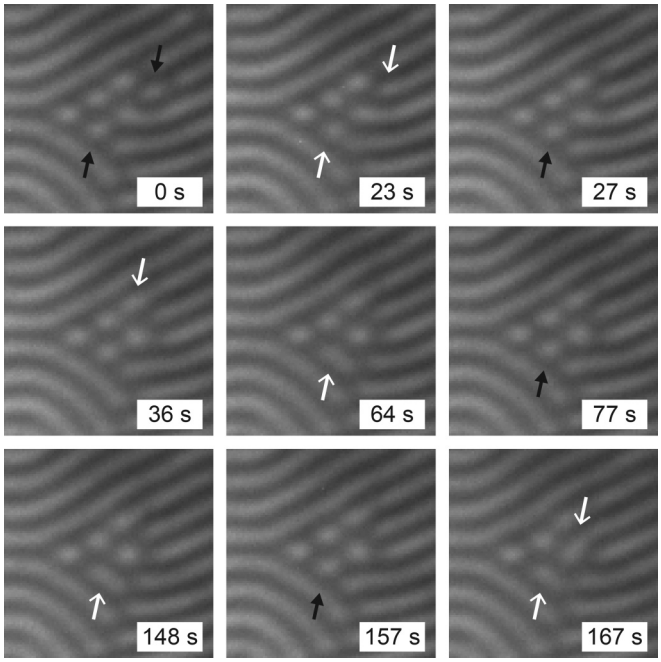

FIG. 4. Time series of Fresnel images of an ordered skyrmion cluster at $T = 243 \pm 0.3$ K. The black and white arrows indicate skyrmions that are formed and annihilated, respectively.

the skyrmions gradually decrease in number from $N = 224$ to 117. At an elevated T, rotation of the ordered skyrmion clusters and oscillation of the stripe terminations right beside the clusters sometimes occur, leading to the breaking of the triangle rule. As a result, the clusters shrink. The rotation at an elevated T and the collective oscillation of the stripes has been reported in Refs. [25,29]. Above ~240 K, the skyrmions rapidly decrease in number, accompanied by rapid restoration of the original stripe domain structures. Eventually, the skyrmions completely disappear at $T_S \sim 254$ K, before T_C of 273 K for thin films [25,27] is reached. Note that N in Fig. 3(a) is counted using the snapshot Fresnel images. The appearance and disappearance of skyrmions, as mentioned later, occur between one measured temperature and the next, and even at fixed temperature, as shown in Fig. 4. Therefore, Fig. 3(a) shows a roughly decreasing trend of skyrmions with increasing temperature. Unexpectedly, the numbers of skyrmions often show an increase, as shown in Fig. 3(b), where ΔN is obtained by subtracting N at a given temperature from that at the next temperature in Fig. 3(a). The spontaneous formation of skyrmions results from a change from the meronlike stripe terminations located next to the clusters to skyrmions, as shown in Fig. 3(c). A triangle-shaped cluster changes size, becoming first larger and then smaller with increasing T. What is more interesting is that skyrmions are selectively formed at HDWs without skyrmions, as shown in Fig. 3(d). At 222 K, a 120° HDW exists without skyrmions. At 223 K a single skyrmion and an HDB appear at the HDW, and then at 230 K the HDB develops. Finally, at 232 K, a 1D skyrmion array is spontaneously formed at the HDW. Such skyrmions are stochastically formed. Note that skyrmions do not appear in the single-Q state without skyrmions (not shown here). Figure 3(e) is a Fresnel image obtained at 252 K just prior to the disappearance of skyrmions by heating shown in Fig. 3(a). Such skyrmions existed only at the HDWs and helimagnetic edge dislocations. These results show that skyrmions and their lattice arrangement correspond to multiple-Q states including the double-Q state and indicate that there is a local minimum-energy state for a skyrmion at HDWs. Note that, as temperature is decreased before reaching T_S, the behavior does not trace the elevated temperature process as in Fig. 3(a) and N is largely unaltered while skyrmions appear and disappear.

The dynamic behavior was also observed at a constant temperature. Figure 4 shows a time series of Fresnel images of an ordered skyrmion cluster at $T = 243 \pm 0.3$ K. The meronlike stripe terminations change to skyrmions and vice versa. This indicates that the helix and skyrmion states are separated by a finite energy barrier under such a zero-field state, and the repeated formation and annihilation is essentially caused by thermal fluctuation.

These behaviors indicate relaxation dynamics. In the whole of a system, the relative probability of a state's realization is generally determined by $\exp(-E/k_B T)$ where E is the state energy and k_B is the Boltzmann constant, i.e., an exponential temperature-dependent change. The transition from stable to metastable state requires higher thermal activation energy than the opposite transition and occurs rarely in the absence of external stimuli. However, we observed that skyrmions are actually excited under the zero-field state even at a low temperature [Fig. 3(b)]. In our FeGe thin films there are two local environments for spontaneous skyrmion formation, i.e., the stripe terminations right beside the clusters [Fig. 3(c)] and the HDWs without skyrmions [Fig. 3(d)]. The spontaneous formation occurs with higher frequency in the former environment, but the two environments generate skyrmions over a wide temperature range. We confirmed that, when the sample is cooled again before reaching T_C after the complete disappearance of skyrmions on heating, skyrmions never appear. Therefore, the unconventional skyrmion excitations under such a zero magnetic field arise from a force that stabilizes skyrmions by the proliferation of topological defects [39], which is supposed to be involved in the helix-to-skyrmion transition, and are not explained only by thermal activation.

To summarize, under a zero magnetic field, after removing the field, we found that skyrmions are trapped and excited at HDWs in FeGe thin films, indicating that skyrmions and their arrangement correspond to multiple-Q states including the double-Q state and there is a local minimum-energy state for skyrmions at HDWs. The unconventional skyrmion excitations at HDWs and the meronlike stripe terminations under such a zero-field state are caused by thermal fluctuation and the force that stabilizes skyrmions by the proliferation of topological defects. These results provide a qualitative explanation of the sign of topological Hall resistivity under a zero magnetic field after removing the field in epitaxial FeGe(111) thin films [27] and may help in understanding of the formation of topological spin textures, probably skyrmions, in the NFL state with partial order under high pressure in MnSi [14–19].

We thank K. Edagawa, M. Mitome, and T. Aizawa for helpful discussions and W. Z. Zhang and H. Usui for technical support during LTEM experiments. This work was

supported by MEXT/JSPS KAKENHI Grants No. 26800195, No. 25289233, No. 26390012, and No. 26420845, the Murata Science Foundation, and the Nanotechnology Platform Project, MEXT, Japan.

[1] A. N. Bogdanov and D. A. Yablonskiĭ, Sov. Phys. JETP **68**, 101 (1989).
[2] A. N. Bogdanov and A. Hubert, J. Magn. Magn. Mater. **138**, 255 (1994).
[3] I. E. Dzyaloshinskii and B. A. Ivanov, JETP Lett. **29**, 540 (1979).
[4] A. S. Kovalev, A. M. Kosevich, and K. V. Maslov, JETP Lett. **30**, 296 (1979).
[5] S. Mühlbauer, B. Binz, F. Jonietz, C. Pfleiderer, A. Rosch, A. Neubauer, R. Georgii, and P. Böni, Science **323**, 915 (2009).
[6] W. Münzer, A. Neubauer, T. Adams, S. Mühlbauer, C. Franz, F. Jonietz, R. Georgii, P. Böni, B. Pedersen, M. Schmidt *et al.*, Phys. Rev. B **81**, 041203(R) (2010).
[7] X. Z. Yu, Y. Onose, N. Kanazawa, J. H. Park, J. H. Han, Y. Matsui, N. Nagaosa, and Y. Tokura, Nature (London) **465**, 901 (2010).
[8] X. Z. Yu, N. Kanazawa, Y. Onose, K. Kimoto, W. Z. Zhang, S. Ishiwata, Y. Matsui, and Y. Tokura, Nat. Mater. **10**, 106 (2010).
[9] N. Nagaosa and Y. Tokura, Nat. Nanotechnol. **8**, 899 (2013).
[10] A. Neubauer, C. Pfleiderer, B. Binz, A. Rosch, R. Ritz, P. G. Niklowitz, and P. Böni, Phys. Rev. Lett. **102**, 186602 (2009).
[11] F. Jonietz, S. Mühlbauer, C. Pfleiderer, A. Neubauer, W. Münzer, A. Bauer, T. Adams, R. Georgii, P. Böni, R. A. Duine *et al.*, Science **330**, 1648 (2010).
[12] T. Schulz, R. Ritz, A. Bauer, M. Halder, M. Wagner, C. Franz, C. Pfleiderer, K. Everschor, M. Garst, and A. Rosch, Nat. Phys. **8**, 301 (2012).
[13] N. Romming, C. Hanneken, M. Menzel, J. E. Bickel, B. Wolter, K. von Bergmann, A. Kubetzka, and R. Wiesendanger, Science **341**, 636 (2013).
[14] S. Tewari, D. Belitz, and T. R. Kirkpatrick, Phys. Rev. Lett. **96**, 047207 (2006).
[15] B. Binz, A. Vishwanath, and V. Aji, Phys. Rev. Lett. **96**, 207202 (2006).
[16] U. K. Rößler, A. N. Bogdanov, and C. Pfleiderer, Nature (London) **442**, 797 (2006).
[17] R. Ritz, M. Halder, M. Wagner, C. Franz, A. Bauer, and C. Pfleiderer, Nature (London) **497**, 231 (2013).
[18] R. Ritz, M. Halder, C. Franz, A. Bauer, M. Wagner, R. Bamler, A. Rosch, and C. Pfleiderer, Phys. Rev. B **87**, 134424 (2013).
[19] H. Watanabe, S. A. Parameswaran, S. Raghu, and A. Vishwanath, Phys. Rev. B **90**, 045145 (2014).
[20] J. Iwasaki, M. Mochizuki, and N. Nagaosa, Nat. Commun. **4**, 1463 (2013).
[21] K. Everschor, M. Garst, R. A. Duine, and A. Rosch, Phys. Rev. B **84**, 064401 (2011).
[22] O. Petrova and O. Tchernyshyov, Phys. Rev. B **84**, 214433 (2011)
[23] M. Mochizuki, Phys. Rev. Lett. **108**, 017601 (2012).
[24] G. Tatara and H. Fukuyama, J. Phys. Soc. Jpn. **83**, 104711 (2014).
[25] M. Nagao, Y. G. So, H. Yoshida, T. Nagai, K. Edagawa, K. Saito, T. Hara, A. Yamazaki, and K. Kimoto, Appl. Phys. Express **8**, 033001 (2015).
[26] K. Ishizuka and B. Allman, J. Electron Microsc. **54**, 191 (2005).
[27] S. X. Huang and C. L. Chien, Phys. Rev. Lett. **108**, 267201 (2012).
[28] M. Uchida, Y. Onose, Y. Matsui, and Y. Tokura, Science **311**, 359 (2006).
[29] M. Uchida, N. Nagaosa, J. P. He, Y. Kaneko, S. Iguchi, Y. Matsui, and Y. Tokura, Phys. Rev. B **77**, 184402 (2008).
[30] C. Pappas, E. Lelièvre-Berna, P. Falus, P. M. Bentley, E. Moskvin, S. Grigoriev, P. Fouquet, and B. Farago, Phys. Rev. Lett. **102**, 197202 (2009).
[31] X. Yu, M. Mostovoy, Y. Tokunaga, W. Zhang, K. Kimoto, Y. Matsui, Y. Kaneko, N. Nagaosa, and Y. Tokura, Proc. Natl. Acad. Sci. USA **109**, 8856 (2012).
[32] S. Seki, X. Z. Yu, S. Ishiwata, and Y. Tokura, Science **336**, 198 (2012).
[33] T. Lancaster, R. C. Williams, I. O. Thomas, F. Xiao, F. L. Pratt, S. J. Blundell, J. C. Loudon, T. Hesjedal, S. J. Clark, P. D. Hatton, M. Ciomaga Hatnean, D. S. Keeble, and G. Balakrishnan, Phys. Rev. B **91**, 224408 (2015).
[34] U. K. Rößler, A. A. Leonov, and A. N. Bogdanov, J. Phys.: Conf. Ser. **303**, 012105 (2011).
[35] M. Ezawa, Phys. Rev. B **83**, 100408 (2011).
[36] R. L. Silva, L. D. Secchin, W. A. Moura-Melo, A. R. Pereira, and R. L. Stamps, Phys. Rev. B **89**, 054434 (2014).
[37] See Supplemental Material at http://link.aps.org/supplemental/10.1103/PhysRevB.92.140415 for details of hysteretic and Temperature-independent helimagnetic domain structures in FeGe thin film.
[38] B. Lebech, J. Bernhard, and T. Freltoft, J. Phys.: Condens. Matter **1**, 6105 (1989).
[39] D. C. Wright, and N. D. Mermin, Rev. Mod. Phys. **61**, 385 (1989).